Transient Cool Down of a Gas in a Closed Container

Jae Min Hyun* and Hoon Ki Choi†
Korea Advanced Institute of Science and Technology, Seoul, Korea

Numerical solutions are obtained for transient natural convection of a compressible fluid in a closed, vertically mounted cylinder at high Rayleigh numbers. Motions are driven by abruptly lowering the temperature at the entire walls of the vessel. The computations simulate some of the recent experiments by Otis and Roesler. Results are presented by solving the full, time-dependent, compressible Navier-Stokes equations. The details of flow and temperature fields in the transient process and their dependence on the relevant parameters are described. When the aspect ratio (height/diameter) is comparable to or smaller than $O(1)$, the evolution of the temperature field is highly oscillatory. The period of oscillation is compatible with that of the internal gravity wave; this is consistent with the previous analytical predictions and experimental observations. The non-Boussinesq fluid effects are shown to be insignificant for the thermal boundary conditions similar to those adopted in the experiments of Otis and Roesler. However, the effects of the thermoacoustic convection are noted, especially in the early-time behavior when the temperature differential is large. Numerically constructed contour maps showing velocity fields are presented to illustrate the distinctive character of the flow structure for extreme values of the cylinder aspect ratio

Introduction

NATURAL convection in a closed cavity at high Rayleigh numbers has been studied extensively. The subject encompasses a wide range of industrial applications, and it entails intrinsic scientific merits (see, e.g., the review article by Ostrach[1]). Most of the previous research has been devoted to the steady-state regimes; only recently has the transient process begun to receive attention. This reflects a recognition that a proper understanding of transient or unsteady phenomena is essential to the design and operation of many technologically innovative fluid-thermal systems.

The significance of convection in the transient adjustment process of a confined, already-stratified fluid to the change in the externally imposed thermal conditions at the container walls has been succinctly pointed out in the context of heat-up (or cool-down) processes (Walin,[2] Sakurai and Matsuda,[3] and Jischke and Doty[4]). Patterson and Imberger[5] envisioned the transient flow of an initially isothermal fluid in a rectangle; the flow was driven by instantaneously raising and lowering the temperature at the respective sidewalls. By relying heavily on scaling arguments and physical insight, they provided a broad classification of the transient regime in terms of the key nondimensional parameters. In line with the preceding analyses, transient buoyant flows in a vessel have been investigated experimentally (Yewell et al.,[6] Ivey,[7] and Otis and Roesler[8]). Also, starting with the classical paper by Wilkes and Churchill,[9] efforts have been expanded to acquire numerical solutions to the full Navier-Stokes equations (Hyun,[10-13] Hyun and Lee,[14] Han,[15] and Markatos and Pericleous[16]). All of these endeavors have considerably deepened our knowledge of the transient dynamics. One notable finding is that the global transient process in the interior core is accomplished over the convective time scale, which is an order of magnitude smaller than the diffusive time scale h^2/κ. Here, h is the characteristic dimension of the container, and κ is the thermal diffusivity of the fluid.

Almost all of the prior work on transient convection has been formulated within the framework of the incompressible Boussinesq-fluid assumptions. This basically ignores the variation of density in the equation of motion other than in the buoyancy term. This approximation is usually adequate to deal with the flow of an incompressible fluid at high Rayleigh numbers. However, the need to use the non-Boussinesq assumption arises when the effect of fluid compressibility is appreciable (Spradley and Churchill[17]). Published accounts that explicitly address the transient behavior of a compressible gas that undergoes convective adjustment processes in a container are scarce.

We now propose to undertake numerical studies of a model problem of a compressible gas in an enclosure. We have selected as the model problem the transient convection of a gas in a cylinder. In part, this study was stimulated by a recent report by Otis and Roesler,[8] who carried out laboratory experiments of cool down using nitrogen gas. They described temperature measurements inside a cylinder of aspect ratio (A = height h/diameter D) of order unity, filled with an initially isothermal (at temperature T_i), motionless nitrogen gas in thermal equilibrium with its external boundaries. The fluid motion was initiated when the temperature of the gas was instantaneously raised to T_f. The subsequent cooling process of the gas, in response to the imposed temperature differential ΔT between the gas and the wall, was monitored by recording temperature histories at several locations near the central axis inside the cylinder. As was ascertained by Ref. 8, these transient temperature data are valuable in view of the lack of experiments using a gas. In scrutinizing the experimental data conducted with ΔT at approximately 40°C, Otis and Roesler raised a question as to whether the non-Boussinesq fluid effects would significantly affect the temperature evolution during the cool-down process of a gas. In the present study, we produced numerical solutions to the full, time-dependent, compressible Navier-Stokes equations without invoking the Boussinesq assumption to examine the cool-down process similar to the experiment of Ref. 8. It was not possible to design numerical calculations that would precisely reproduce the experiments of Ref. 8. Therefore, the numerical results were obtained in somewhat different parameter regimes from those of Ref. 8. The objectives here were to attempt qualitative comparisons with the experimental finding, thereby helping to form a proper perspective of the transient process under consideration. All of the terms in the equations were retained. By executing a series of comprehensive and systematic numerical simulations, details of the flow and thermal structures were acquired. We also intended to perform extensive parametric studies to isolate the explicit effects of the relevant physical variables. Numerical results have been

Received May 26, 1988; revision received Oct. 13, 1988.

*Professor, Department of Mechanical Engineering. Member AIAA.

†Graduate Student, Department of Mechanical Engineering.

compiled for the Rayleigh number $R_{a_h} = 10^5 \sim 10^9$ for the cylinder aspect ratio $A = 0.05 \sim 20$.

Another motivation behind the present study was to delineate, by way of conducting numerical simulations, the existence of the propagating temperature front and the oscillatory approach to steady state in the cool-down process of a gas. For the case of heat up (or cool down) of an incompressible Boussinesq fluid from an initially isothermal quiescent state, it has been observed that the transient thermal structure in the interior core is divided into two regions by a vertically propagating temperature front (Hyun,[10–13] and Rahm and Walin[18]). The fluid ahead of the front retains the original uniform temperature; the fluid behind the front becomes stratified. The current numerical solutions portray the propagating front, which is in qualitative accord with the measurements by Ref. 8. The temperature information presented by the experiments of Ref. 8 clearly displayed the oscillatory approach to steady state. This transient behavior is consistent with the theoretical prediction derived by Patterson and Imberger.[5] It has been asserted in Ref. 5 that if $R_a > P_r^4 A^{-4}$ [where R_a is the system Rayleigh number, P_r the Prandtl number, and A the aspect ratio (height/width) of the rectangular cavity], the approach to steady state would be oscillatory due to the presence of internal gravity waves. The issue regarding the existence of such an oscillatory approach has been extensively discussed in the recent literature (Yewell et al.,[6] Ivey,[7] and Patterson[19]). We shall inspect the temperature data generated by the present numerical simulations. The numerical results for the cases of $A \sim O(1)$ clearly depict oscillatory approaches to the steady state.

The prior work, including the experiment in Ref. 8, has mainly been concerned with the cases of the cavity aspect ratio $A \sim O(1)$. The character of transient convection for extreme values of the aspect ratio, i.e., $A \gg 1$ and $A \ll 1$, for a compressible gas in a container has not been fully explored in the literature. We will report on the preliminary results of the numerical calculations for $A \gg 1$ and $A \ll 1$. The distinctly different flow properties for these cases will be displayed, and plausible physical mechanisms responsible for this behavior will be discussed.

In summary, the major purpose of this study is to depict the cool-down process of a compressible gas by solving the compressible Navier-Stokes equations without invoking the Boussinesq-fluid assumptions. The numerical results are found to be qualitatively consistent with the laboratory measurements of Ref. 8. For the experimental conditions qualitatively similar to Ref. 8, the numerical results are supportive of the theoretical contentions derived under the Boussinesq-fluid approximation.

The Model

Consider a vertically mounted circular cylinder of radius $D/2$ and height h filled with nitrogen gas. Initially, the gas is at rest in thermal equilibrium at uniform temperature T_0. At $t = 0$, the temperature at the entire cylinder wall is abruptly lowered to T_w, and is maintained thereafter. The subsequent adjustment process of the gas, due to the temperature differential $\Delta T_0 = T_0 - T_w$, is to be described. We assume a compressible, viscous, and heat-conducting gas that obeys the ideal gas law. The relevant physical properties of the gas are thermal conductivity k, dynamic viscosity μ, and specific heat C_p.

The motion will be governed by the full, axisymmetric, time-dependent compressible Navier-Stokes equations. Referred to a cylindrical coordinate frame (r,z) with corresponding velocity components (u,w), these equations are, using standard notations,

$$\frac{\partial \rho}{\partial t} + \frac{1}{r}\frac{\partial}{\partial r}(\rho r u) + \frac{\partial}{\partial z}(\rho w) = 0$$

$$\frac{\partial}{\partial t}(\rho u) + \frac{1}{r}\frac{\partial}{\partial r}(\rho r u u) + \frac{\partial}{\partial z}(\rho u w) - \frac{\partial}{\partial z}\left(\mu \frac{\partial u}{\partial z}\right) - \frac{1}{r}\frac{\partial}{\partial r}\left(\mu r \frac{\partial u}{\partial r}\right) = -\frac{\partial p}{\partial r} + \frac{1}{r}\frac{\partial}{\partial r}\left(\mu r \frac{\partial u}{\partial r}\right) - 2\mu\frac{\mu}{r^2} - \frac{2}{3r}\frac{\partial}{\partial r}(\mu r \nabla \cdot q) + \frac{\partial}{\partial z}\left(\mu \frac{\partial w}{\partial r}\right)$$

$$\frac{\partial}{\partial t}(\rho w) + \frac{1}{r}\frac{\partial}{\partial r}(\rho r u w) + \frac{\partial}{\partial z}(\rho w w) - \frac{\partial}{\partial z}\left(\mu \frac{\partial w}{\partial z}\right) - \frac{1}{r}\frac{\partial}{\partial r}\left(\mu r \frac{\partial w}{\partial r}\right) = -\frac{\partial p}{\partial z} + \frac{\partial}{\partial z}\left(\mu \frac{\partial w}{\partial z}\right) + \frac{1}{r}\frac{\partial}{\partial r}\left(\mu r \frac{\partial u}{\partial z}\right) - \frac{2}{3}\frac{\partial}{\partial z}\left(\mu \nabla \cdot q\right) - \rho g$$

$$\frac{\partial}{\partial t}(\rho H) + \frac{1}{r}\frac{\partial}{\partial r}(\rho r u H) + \frac{\partial}{\partial z}(\rho w H) = \frac{1}{r}\frac{\partial}{\partial r}\left(\frac{k}{C_p} r \frac{\partial H}{\partial r}\right) + \frac{\partial}{\partial z}\left(\frac{k}{C_p}\frac{\partial H}{\partial z}\right) + \frac{\partial p}{\partial t}$$

$$P = \rho Q T$$

where

$$\nabla \cdot q = \frac{1}{r}\frac{\partial}{\partial r}(ru) + \frac{\partial w}{\partial z}, \qquad H = C_p T$$

and Q denotes the gas constant. The initial conditions are

$$u = w = 0$$

$$T = T_0, \qquad \rho = \rho_0,$$

at $t = 0$.

The boundary conditions are

$$u = w = 0, \qquad T = T_w$$

at all walls.

In order to account for the temperature dependency of the dynamic viscosity, the well-known Sutherland formula is adopted (in mks units, T in degrees Kelvin):

$$\mu = 1.4 \times 10^{-6} \times T^{3/2} \times \frac{1}{T + 106.7}$$

The following nondimensional parameters are relevant (e.g., Ostrach[1] and Spradley and Churchill[17]):

$$A = \frac{h}{D}, \text{ aspect ratio}$$

$$R_{a_h} = \frac{g\,\Delta\rho_0 h^3 \rho_0^2 C_p}{\rho_w \mu_0 k_0}, \text{ Rayleigh number based on height}$$

$$R_{a_D} = \frac{R_{a_h}}{A^3}, \text{ Rayleigh number based on diameter}$$

$$P_r = \frac{C_p \mu_0}{k_0}, \text{ Prandtl number}$$

$$Re = \frac{\rho_w D (Q\,\Delta T_0)^{1/2}}{\mu_w}, \text{ acoustic Reynolds number}$$

and $\Delta\rho_0 = \rho_w - \rho_0$, where subscripts 0 and w refer to the values in the intial state and the wall conditions, respectively. The significance of Re will be evident in connection with the effects of thermoacoustic convection.[17]

In order to solve the preceding system of equations, we have used the finite-difference procedures. After having undergone trial calculations using several finite-difference algorithms, we constructed a code based on the SIMPLE-type approach originally developed by Patankar.[20] This numerical method is well established, and the specifics of the numerical techniques underlying SIMPLE are amply documented in Patankar[20] and elsewhere. The equations were finite-differenced using the primitive variables on a staggered grid, and the corrections for the pressure terms were made following the guidelines given in Ref. 20. Sensitivity tests to the grid size were made and the results were satisfactory. Grid stretchings in both directions were incorporated in the codes to ensure adequate resolution of the boundary layers. Most of the computations were conducted using a [27 × 27] mesh for the case of $A \sim O(1)$. For the cases of extreme values of A, appropriately larger numbers of mesh points were used to describe the flowfields.

The results of numerical computations will now be presented. In the following figures, the dimensionless quantities are introduced.

$$R = \frac{r}{D/2}, \qquad Z = z/h$$

$$\theta = \frac{T - T_w}{\Delta T_0}, \qquad \tau = t/t_h$$

The nondimensionalization of time was guided by the prior analyses on linear heat up[3,4]; the heat up time scale t_h is defined as

$$t_h = 2^{-1/2} P_r^{1/2} R_{a_h}^{1/4} N_0^{-1} D/2\, h$$

where $N_0 = (g\, \Delta\rho_o/h\rho_w)^{1/2}$, the Brunt-Väisäla frequency characterizing the overall strength of stratification.

As mentioned earlier, the discussion will be centered on the evolutions of temperature and velocity fields. Only the results that bring into focus the explicit effects of the relevant parameter will be illustrated.

The current numerical computations were not designed to reproduce precisely the experiments of Ref. 8. In the experiments, the gas was initially compressed up to a pressure of 100 atm over a time interval of 1 s or less. Accordingly, the gas temperatures rise rapidly during the compression stroke, and the time zero coincides with the instant of the maximum gas temperatures attained at the final stage of the compression stroke. The current numerical calculations did not intend to reproduce exactly the extremely complicated processes encountered in the experiments. Instead, the aim was to bring into focus the essential dynamic mechanisms responsible for the overall cool down of the interior gas. Therefore, an idealized model was selected for detailed numerical investigations. In the simplified numerical model considered in the present paper, the nitrogen gas at the initial state was assumed to be in thermal equilibrium at 5 atm. For all the calculations reported here, $P_r = 0.72$.

Results and Discussion

Time histories of the temperature field at several selected locations will be scrutinized. The numerical results for the temperature evolution will play a role similar to the temperature traces obtainable from the output of thermocouples in the laboratory experiments of Ref. 8. These data are useful in confirming the existence of the temperature front and of an oscillatory approach to steady state. The major findings of the experiments of Ref. 8 are also presented by using charts showing the temperature histories at several locations near the axis.

Figures 1 and 2 show time histories in a cylinder with aspect ratio $A = 1$ for two values of R_{a_h}. The temperature difference used for these computations was $\Delta T_0 = 40$ K (i.e., $T_0 = 340$ K, $T_w = 300$ K). It is apparent that the overall transient phase is substantially accomplished over the heat-up time scale, i.e., $\tau \sim O(1)$, which is in accord with the results of Refs. 3, 4, and 10–13. This suggests that the convective heat-up time scale t_h, which was assessed under the Boussinesq assumption, is still applicable in characterizing the overall adjustment of a compressible fluid under the present circumstances.

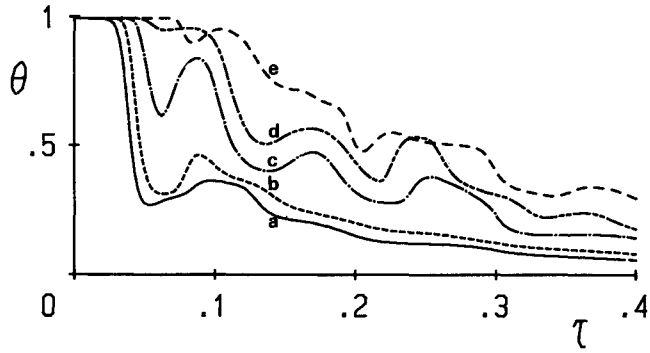

Fig. 1 Plots of temperature evolution near the axis ($R = 0.1$). $R_{a_h} = 5.30 \times 10^7$, $R_{a_D} = 5.30 \times 10^7$, $h/D = 1$, $\Delta T_0 = 40$ K. The vertical positions are a) ———, $Z = 0.12$; b) ------, $Z = 2.23$; c) – – – –, $Z = 0.40$; d) –·–·–, $Z = 0.55$; e) - - - - -, $Z = 0.77$.

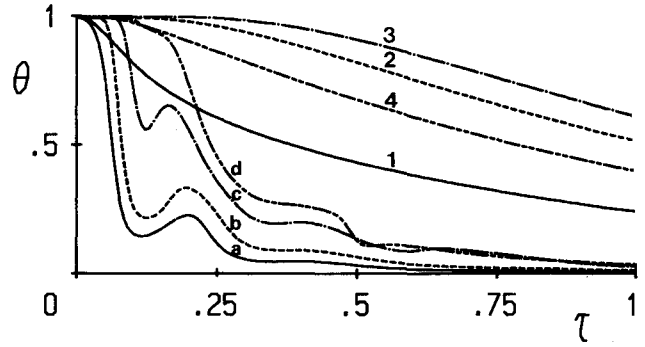

Fig. 2 Plots of temperature evolution near the axis ($R = 0.1$). $R_{a_h} = 3.40 \times 10^6$, $R_{a_D} = 3.40 \times 10^6$, $h/D = 1$, $\Delta T_0 = 40$ K. The vertical positions are a) ———, $Z = 0.10$; b) ------, $Z = 0.28$; c) – – – –, $Z = 0.59$; d) –·–·–, $Z = 0.80$. Curves 1–4 show the results for $g = 0$. the vertical positions are 1) ———, $Z = 0.10$; 2) - - - - - -, $Z = 0.28$; 3) –·–·–, $Z = 0.59$; 4) –··–··–, $Z = 0.80$.

In order to demonstrate the overwhelming influence of buoyant convective activities in comparison to that of nonbuoyant effects, sample calculations have been made by setting $g = 0$ in the governing equations. The results will isolate the dynamic effects exclusive of the buoyancy-driven convection. Curves 1–4 in Fig. 2 depict temperature histories representative of such results. It is obvious that all of the nonbuoyancy effects are very small in bringing about the global cooling down in the fluid interior. The nonbuoyancy effects include principally conduction and the pressure-driven thermoacoustic convection.[17]

In order to gage the importance of the individual nonbuoyancy effect, the conduction equation was solved. The results of the conduction solutions were similar to the solutions of the Navier-Stokes equations obtained by setting $g = 0$, i.e., curves 1–4 of Fig. 2. This indicates that, for the conditions of Fig. 2 with $\Delta T_0 = 40$ K, conduction is the dominant heat-transfer mode among the nonbuoyant effects, and thermoacoustic convection is insignificant. However, as will be illustrated later, the comparative importance of thermoacoustic convection increases when the temperature differential ΔT_0 takes a substantially large value (see Fig. 3 for $g = 0$, $\Delta T_0 = 600$ K).

In summary, the overall results shown in Figs. 1 and 2 confirm that, under the physical conditions considered in the present calculations, the predominant ingredient in the transient process is buoyant convection.

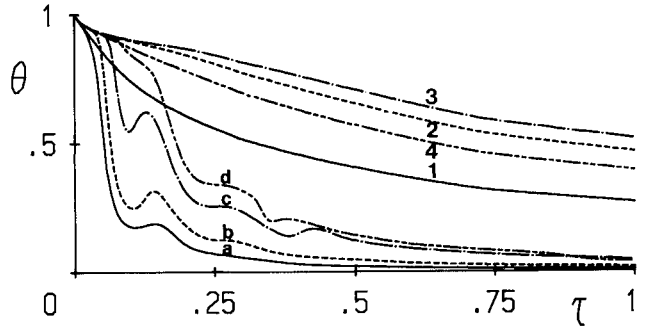

Fig. 3 Plots of temperature evolution near the axis ($R = 0.1$). $R_{a_h} = 7.50 \times 10^5$, $R_{a_D} = 7.50 \times 10^5$, $h/D = 1$, $\Delta T_0 = 600$ K. The vertical positions are a) ———, $Z = 0.10$; b) ------, $Z = 0.28$; c) – – – –, $Z = 0.59$; d) –·–·–, $Z = 0.80$. Curves 1–4 show the results for $g = 0$. The vertical positions are 1) ———, $Z = 0.10$; 2) - - - - - -, $Z = 0.28$; 3) – – – – –, $Z = 0.59$; 4) –·–·–, $Z = 0.80$.

The presence of the vertically upward propagating temperature front is also clearly captured in Figs. 1 and 2. As expounded in Refs. 8, 10–13, and 18, the temperature at a given location in the interior does not change until the arrival of the fluid particle that has traveled through the boundary layer and returned to the interior. Ahead of this front, the fluid remains nonstratified, retaining the original uniform temperature of the initial state. Behind the front, the stratifying process takes place. It is noteworthy in Figs. 1 and 2 that the temperature curves remain constant until they are engulfed sequentially by the temperature front. It will be ascertained later (see Fig. 3) that the temperatures in the interior change even prior to the arrival of the temperature front, if the thermoacoustic effects are appreciable. The results in Figs. 1 and 2 indicate that the time for the front to traverse the height of the container t_f scales with $t_f \leq O(t_h)$. As R_{a_h} decreases, the propagation speed of the front increases. The facilitation of the cool-down process at lower values of R_{a_h} is more pronounced in the region well behind the front and at large times. These are attributable to the enhanced role of the diffusive effects as R_{a_h} decreases.[11,12]

Another issue of much current interest is the existence of an oscillatory approach to steady state. The classical analysis of Ref. 5 predicted an oscillatory behavior in transient natural convection in a rectangle in the flow regime $P_r^4 A^{-4} < R_{a_h}$. This issue has been debated extensively in the recent literature.[6,7,19] In particular, we note that the recent experimental measurements in Ref. 8 using nitrogen gas clearly revealed an oscillatory approach to steady state. Patterson and Imberger[5] theorized that this oscillatory behavior reflected the system-scale internal gravity wave activities. They continued to argue that the period of oscillation t_0 should be compatible with the period of internal gravity wave t_i given as

$$t_i \sim 2\pi(A^2 + 1)^{1/2}/N_0 \qquad (1)$$

The computed results shown in Figs. 1 and 2 clearly exhibit a distinct transient oscillatory approach to steady state. For the run of Fig. 1, the period of oscillations detectable in the temperature traces, expressed in nondimensional quantities, are $t_0 \approx 0.075 \sim 0.093$. Equation (1) gives $t_i \approx 0.078 \sim 0.116$. In a similar fashion, we have found, for the run in Fig. 2, $t_0 \approx 0.22 \sim 0.253$, and $t_i \approx 0.194 \sim 0.247$. The preceding comparisons of t_i and t_0 clearly establish that, for the flows considered, the transient phase is oscillatory and the periods of oscillation are comparable to the periods of internal gravity waves. The effect of R_{a_h} on the oscillatory behavior is also discernible. For a lower value of R_{a_h}, convection is less vigorous and, consequently, the oscillatory behavior weakens by the diffusive damping (see Fig. 2). It is apparent in Fig. 1 that, as R_{a_h} increases, the oscillatory behavior is more distinct and survives over a longer time. Further, the numerical results in Figs. 1 and 2 reveal that the temperature evolution is less oscillatory in the regions close to the endwalls. This is ascribed to the influence of the diffusive effects near the end walls, which damp out the oscillatory activities.

In summary, the temperature histories for $A = 1$ illustrated in Figs. 1 and 2 corroborate the theoretical contentions of Ref. 5 and the experimental measurements of Ref. 8.

The previously discussed results of numerical computations for a compressible gas are in broad qualitative agreement with the predictions based on the Boussinesq-fluid assumptions. The explicit compressibility effects have not been noticeable in Figs. 1 and 2. We point out that the results shown in Figs. 1 and 2 are obtained using a relatively small temperature differential: $\Delta T_0 = 40$ K. As mentioned for Fig. 2, the nonbuoyancy effects are dominated by the ubiquitous conduction for these conditions; the thermoacoustic effects, which are appreciable when the compressibility effects are substantial, have been insignificant.

Now, we shall demonstrate the flow conditions under which the specific effects of the compressibility are pronounced. Figure 3 presents the numerical results when the temperature differential is substantially large, i.e., $\Delta T_0 = 600$ K ($T_0 = 900$ K, $T_w = 300$ K). Curves a–d denote the temperature histories for normal gravity ($g = 9.8$ m-s^{-2}), whereas curves 1–4 show the data for $g = 0$ in order to emphasize the nonbuoyancy effects. It is readily discernible in curves a–d of Fig. 3 that the temperatures at early times decrease even prior to the arrival of the temperature front. This early-time behavior is in contrast to the data shown in Figs. 1 and 2 in which the temperatures remain unchanged until the arrival of the temperature front.

Inspection of the temperature data for normal gravity (curves a–d) and those obtained for $g = 0$ (curves 1–4) in Fig. 3 leads to the observation that the nonbuoyancy effects are noticeable, especially at early times. For a breakdown of the nonbuoyancy effects, the conduction equation was solved. The conduction solutions were quite similar to curves 1–4 of Fig. 2 (there were minor differences owing to the small differences in thermophysical properties used). These comparisons indicate that the thermoacoustic convection is an effective mechanism to help achieve the overall cool-down process. In particular, the early-time temperature drops in the interior points far away from the walls, even prior to the arrival of the temperature front, are largely attributable to the thermoacoustics effects. Physically speaking, the sudden cooling in the boundary layers near the walls causes the gas in the boundary layers to shrink in volume. This brings about a concomitant increase of the volume occupied by the interior gas. Consequently, the essentially inviscid interior gas undergoes an adiabatic expansion, and the interior gas temperature falls.[8] These thermoacoustic effects are conspicious, especially at early times when the buoyancy-driven convective flows are still not fully established. As pointed out in Refs. 8 and 17, this feature is not expected in the usual Boussinesq-fluid convections or, as depicted in Figs. 1 and 2, in the situations in which the compressibility is insignificant.

Summarizing the results shown in Figs. 1–3, the nonbuoyancy effects, especially the thermoacoustic convection, can be an appreciable contributor to the global transient cool-down process at early times. In view of the sonic nature of the thermoacoustic convection, these compressible-fluid effects become more pronounced when the temperature differential is substantially large. As introduced in Ref. 17, the relative importance of the thermoacoustic effects in compressible-fluid flows can be measured by using a parameter like the acoustic Reynolds number Re. We consider the cases in which the wall conditions are assumed to be the same; we have used $Re = 1.4 \times 10^6$ for Fig. 2, and $Re = 5.4 \times 10^6$ for Fig. 3. The previously stated considerations emphasize the need of introducing an additional suitably defined parameter such as Re, which would denote the influence of the compressibility in describing the cool-down process in which the compressibility is prominent.

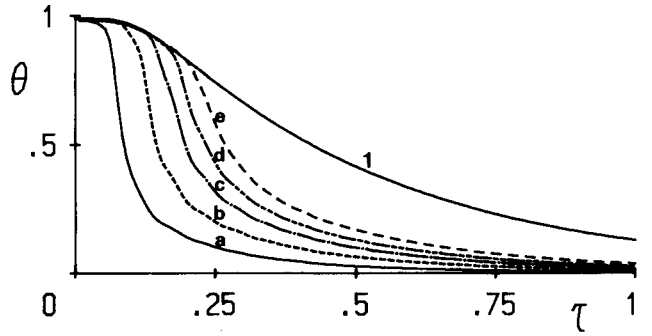

Fig. 4 Plots of temperature evolution near the axis ($R = 0.1$). $R_{a_h} = 3.40 \times 10^9$, $R_{a_D} = 4.26 \times 10^5$, $h/D = 20$, $\Delta T_0 = 40$ K. The vertical positions are a) ———, $Z = 0.04$; b) ------, $Z = 0.17$; c) – – – – –, $Z = 0.33$; d) –·–·–, $Z = 0.50$; e) - - - - - -, $Z = 0.68$. Curve 1 shows the result for $g = 0$. The vertical position for curve 1 is ———, $Z = 0.50$.

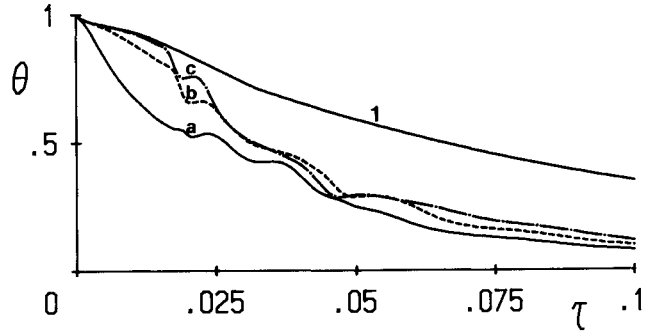

Fig. 5 Plots of temperature evolution near the axis ($R = 0.05$). $R_{a_h} = 4.26 \times 10^5$, $R_{a_D} = 3.40 \times 10^9$, $h/D = 0.05$, $\Delta T_0 = 40$ K. The vertical positions are a) ———, $Z = 0.19$; b) ------, $Z = 0.50$; c) – – – – –, $Z = 0.73$. Curve 1 shows the result for $g = 0$. The vertical position for curve 1 is ———, $Z = 0.50$

We shall now examine the effect of the aspect ratio. Figure 4 shows the temperature histories for large aspect ratios, i.e., $A \gg 1$. It is immediately clear that the convective activities in the core, driven by the boundary-layer flows at the sidewall, are the dominant mechanism to effect the cooling process. Again, the overall adjustment process is substantially accomplished over t_h. However, conduction from the sidewall is not insignificant; Fig. 4 clearly shows that the temperature near the central axis begins to fall even before the location is engulfed by the temperature front. For a cylinder with $A \gg 1$, conduction from the top and bottom endwall disks is minor compared to that from the sidewall. Accordingly, under the assumption of an infinite cylinder, the temperature evolution near the central axis caused by conduction is plotted in Fig. 4. Although the conductive contribution at a given location persists over the entire transient process, the conductive effects are overwhelmed by the convective effects after the passage of the front. Therefore, the temperature change caused by conduction is less conspicuous after the passage of the front.

Figure 5 is representative of the temperature behavior when $A \ll 1$. In this case, the convective circulation driven by the sidewall boundary-layer flow is ineffective in causing the temperature change in the interior. The fluid at a given location is heavily influenced by conduction from the top and bottom endwall disks. Even before the convective flows reach the location, the temperature has fallen substantially by the conductive mechanism. Noting that $A \ll 1$, the temperature behavior with time resulting from conduction along the central axis can be readily computed by use of the Heisler chart, assuming conduction occurs between two parallel infinite plates. The temperature changes caused by conduction are over-plotted in Fig. 5. It is apparent in Fig. 5 that the global temperature adjustment process is completed over a time span that is much smaller than t_h. It should be recalled that t_h has

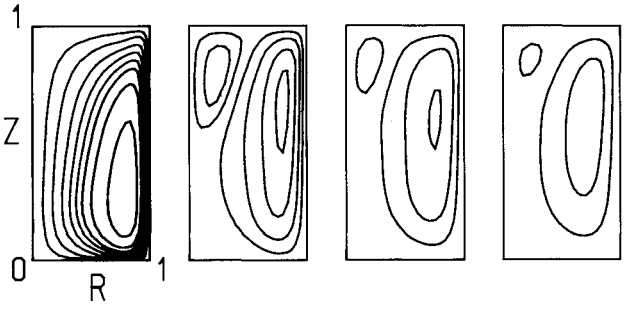

Fig. 6 Contour plots of ψ in the meridional plane. $R_{a_h} = 3.40 \times 10^6$, $R_{a_D} = 3.40 \times 10^6$, $h/D = 1$, $\Delta T_0 = 40$ K. Times are a) $\tau = 0.07$; b) $\tau = 0.68$; c) $\tau = 1.02$; d) $\tau = 1.36$.

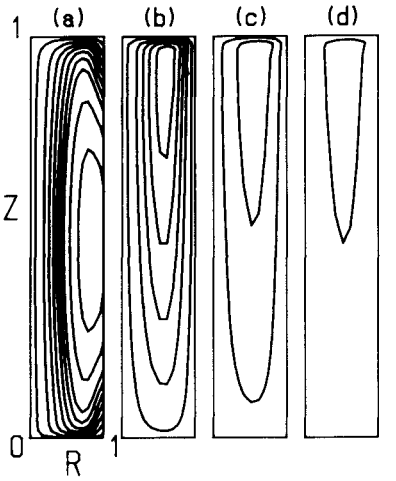

Fig. 7 Contour plots of ψ in the meridional plane. $R_{a_h} = 3.40 \times 10^9$, $R_{a_D} = 4.26 \times 10^5$, $h/D = 20$, $\Delta T_0 = 40$ K. Times are a) $\tau = 0.15$; b) $\tau = 0.57$; c) $\tau = 0.96$; d) $\tau = 1.54$. The figures are stretched in the radial direction to enhance clarity.

been computed by adopting R_{a_h}, rather than R_{a_D}, as the characteristic Rayleigh number in the formulation.

In an effort to gain further physical insight into the dynamics, the approximate form of meridional circulation patterns are demonstrated by plotting the stream function ψ in Figs. 6–8. Here, ψ is defined such that $\rho u = (1/r)(\partial\psi/\partial z)$, $\rho w = -(1/r)(\partial\psi/\partial r)$. Strictly speaking, the problem entails an unsteady compressible fluid flow, thus the exact form of the continuity equation includes the $\partial\rho/\partial t$ term. However, for the entire set of the cases computed, examination of the flow data reveals that the magnitude of $\partial\rho/\partial t$ is substantially smaller (usually less than 1%) than that of $\partial\rho u/\partial r$ or $\partial\rho w/\partial z$. Therefore, plots of the previously defined function ψ depict the approximate patterns of the mass flow structure. Figure 6 presents exemplary plots for the case of $A = 1$. At early times, a clockwise cell forms near the sidewall, driven by the downward flow in the sidewall boundary layer. At small and intermediate times, the clockwise circulation, induced by the sidewall boundary layer, intensifies. At the same time, in the upper region near the central axis, the fluid is cooled from above. The fluid of low temperature, thus of higher density, sinks, and this causes another clockwise circulation cell located in the upper inner region of the flowfield. At large times, as the process has progressed, these convective activities diminish accordingly. The smoothing out of the remaining small nonuniformities in the flow takes place over the diffusive time scale $R_{a_h}^{1/2} N_0^{-1}$, which is an order of magnitude larger than the convective time scale t_h.

For a cylinder of large aspect ratio i.e., $A \gg 1$, the circulation patterns show distinctly different features as compared to those for $A \sim O(1)$. As is discernible in Fig. 7, the circulation

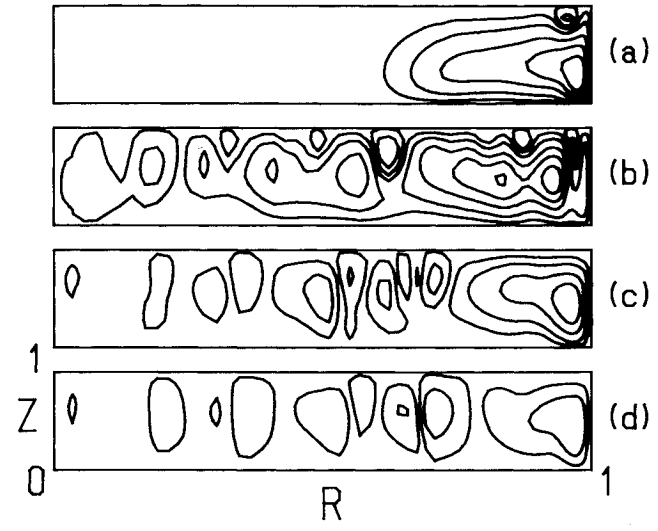

Fig. 8 Contour plots of ψ in the meridional plane. $R_{a_h} = 4.26 \times 10^5$, $R_{a_D} = 3.40 \times 10^9$, $h/D = 0.05$, $\Delta T_0 = 40$ K. Times are a) $\tau = 0.016$; b) $\tau = 0.060$; c) $\tau = 0.100$; d) $\tau = 0.160$. The figures are stretched in the axial direction to enhance clarity.

patterns for $A \gg 1$ are characterized by a one-cell structure. A dominant cell is seen near the sidewall; this cell, which is stretched over the entire height of the cylinder, fills most of the interior of the container.

Figure 8 illustrates the circulation patterns for $A \ll 1$. It is also interesting to note that in the regions close to the top end-wall disk, say $Z \geq 0.5$, the transient situation is akin to a fluid layer cooled from above. This is suggestive of a Benard-type configuration, which may lead to gravitational instability under appropriate conditions. At small times, the Benard-like convective motions are visible in the upper region of the fluid layer over the entire radius of the cylinder. As time elapses, this multicell, Benard-type convection strengthens in magnitude. At large times, as the interior fluid cools down, the convective motions gradually diminish with time.

In summary, the calculations reported in the present study encompass the physical system qualitatively similar to the laboratory experiments of Otis and Roesler. Therefore, the computations performed by using the non-Boussinesq fluid assumptions have recovered most of the features that are anticipated under the conventional Boussinesq assumption, when the thermoacoustic effects are minor. However, the thermoacoustic convection can be an appreciable contributor to the cool-down process of a gas at early times if the temperature differential is substantially large.

Conclusions

Numerical solutions have been obtained of the cool-down process of a compressible fluid in a vertically mounted cylinder. Under conditions qualitatively similar to the experiments of Otis and Roesler, the temperature histories show distinct oscillatory behavior. In accord with the earlier predictions, the period of oscillation is comparable to the period of internal gravity waves. The vertically propagating temperature front is clearly captured.

The explicit effect of the non-Boussinesq fluid approximation is insignificant, if the temperature differential is moderate. The computed time histories are qualitatively consistent with the analytical predictions and the experimental data. However, the nonbuoyancy effects, in particular the thermoacoustic convection, can be appreciable in realizing the cool down process at the early times if the temperature differential is substantially large.

The effects of the container aspect ratio A are shown to be noticeable. For A comparable to or larger than $O(1)$, the buoyancy-driven convection is the dominant mechanism. For A much smaller than $O(1)$, the conductive heat transfer from the end-wall disks plays a major role.

The transient flow patterns are demonstrated to illustrate how the character of flow is affected by A. For $A \gg 1$, a one-cell structure persists over most of the time. For $A \sim O(1)$ at small and intermediate times, a two-cell structure is seen. For $A \ll 1$ at intermediate times, Benard-like multicell flow patterns are obtained.

Acknowledgment

This work was supported in part by a research grant from the Korea Science and Engineering Foundation. The authors are grateful to the anonymous referees of this paper. Their constructive and useful suggestions have led to improvements in the paper.

References

[1]Ostrach, S., "Natural Convection Heat Transfer in Cavities and Cells," *Proceedings of the 7th International Heat Transfer Conference Munich*, Vol. 1, Hemisphere, Washington, DC, 1982, pp. 365–379.

[2]Walin, G., "Contained Non-Homogeneous Flow Under Gravity or How to Stratify a Fluid in the Laboratory," *Journal of Fluid Mechanics*, Vol. 48, Aug. 1971, pp. 647–672.

[3]Sakurai, T. and Matsuda, T., "A Temperature Adjustment Process in a Boussinesq Fluid via a Buoyancy Induced Meridional Circulation," *Journal of Fluid Mechanics*, Vol. 54, No. 3, Aug. 1972, pp. 417–421.

[4]Jischke, M. C. and Doty, R. T., "Linearized Buoyant Motion in a Closed Container," *Journal of Fluid Mechanics*, Vol. 71, No. 4, Oct. 1975, pp. 729–754.

[5]Patterson, J. and Imberger, J., "Unsteady Natural Convection in a Rectangular Cavity," *Journal of Fluid Mechanics*, Vol. 100, No. 1, Nov. 1980, pp. 65–86.

[6]Yewell, R., Poulikakos, D., and Bejan, A., "Transient Natural Convection Experiments in Shallow Enclosure," *Transactions of the ASME, Journal of Heat Transfer*, Vol. 104, Aug. 1982, pp. 533–538.

[7]Ivey, G. N., "Experiments on Transient Natural Convection in a Cavity," *Journal of Fluid Mechanics*, Vol. 144, July 1984, pp. 389–401.

[8]Otis, D. R. and Roesler, J., "Development of Stratification in a Cylindrical Container," *International Journal of Heat and Mass Transfer*, Vol. 30, Aug. 1987, pp. 1633–1638.

[9]Wilkes, J. O. and Churchill, S. W., "The Finite-Difference Computation of Natural Convection in a Rectangular Enclosure," *AIChE Journal*, Vol. 12, 1966, pp. 161–166.

[10]Hyun, J. M., "Transient Process of Thermally Stratifying an Initially Homogeneous Fluid in an Enclosure," *International Journal of Heat and Mass Transfer*, Vol. 27, Oct. 1984, pp. 1936–1938.

[11]Hyun, J. M., "Transient Buoyant Convection of a Contained Fluid Driven by the Changes in the Boundary Temperature," *Transactions of the ASME, Journal of Applied Mechanics*, Vol. 52, March 1985, pp. 193–198.

[12]Hyun, J. M., "Thermally-Forced Stratification Build-Up in an Initially Isothermal Contained Fluid," *Journal of Physical Society of Japan*, Vol. 54, March 1985, pp. 942–949.

[13]Hyun, J. M., "Effect of the Prandtl Number on Heat-Up of a Stratified Fluid in an Enclosure," *Transactions of the ASME, Journal of Heat Transfer*, Vol. 107, Nov. 1985, pp. 982–984.

[14]Hyun, J. M. and Lee, J. W., "Transient Natural Convection in a Square Cavity of a Fluid with Temperature-Dependent Viscosity," *International Journal of Heat and Fluid Flow*, Vol. 9, No. 3, Sept. 1988, pp. 278–285.

[15]Han, S. M., "A Transient Numerical Analysis of Heated Square Cavity," American Society of Mechanical Engineers, Paper 84-HT-57, 1984.

[16]Markatos, N. C. and Pericleous, K. A., "Laminar and Turbulent Natural Convection in an Enclosed Cavity," *International Journal of Heat and Mass Transfer*, Vol. 27, May 1984, pp. 755–772.

[17]Spradely, L. W. and Churchill, S. W., "Pressure- and Buoyancy-Driven Thermal Convection in a Rectangular Enclosure," *Journal of Fluid Mechanics*, Vol. 70, No. 4, Aug. 1975, pp. 705–720.

[18]Rahm, L. and Walin, G., "On Thermal Convection in Stratified Fluids," *Geophysics, Astrophysics and Fluid Dynamics*, Vol. 13, 1979, pp. 51–65.

[19]Patterson, J., "On the Existence of an Oscillatory Approach to Steady Natural Convection in Cavities," *Transactions of the ASME, Journal of Heat Transfer*, Vol. 106, Feb. 1984, pp. 104–108.

[20]Patankar, S. V., *Numerical Heat Transfer and Fluid Flow*, McGraw-Hill, New York, 1980, pp. 41–137.